

ALPHA Progress 2023

J.S. Hangst for the ALPHA Collaboration

Results from earlier runs

The major breakthrough of the ALPHA experiment for 2023 was the publication of the first-ever observation of the effect of gravity on the motion of antimatter¹. The data for this article were taken during the 2022 run. This result, from the new ALPHA-g experiment, was published in *Nature* on 27 September. We were able to demonstrate that atoms of antihydrogen are attracted to the Earth in a manner consistent with the behaviour of normal matter. This measurement, long a goal of the physics program at the AD complex, is the first step in the study of the gravitational nature of antimatter. In future experiments, we will improve the precision (currently about 20%) of the measured acceleration of antihydrogen atoms in the field of the Earth. See the slides for a brief summary of the experiment.

A second result, reporting the first analysis of 1S-2S spectroscopy on antihydrogen atoms that have been laser cooled², has been accepted for publication in *Nature Physics*. This article describes the first spectroscopy on both of the hyperfine components of the 1S-2S transition, and it considers the implications for various parameters of the Standard Model Extension framework.

A third article, describing measurement and modelling of so-called patch potentials in ALPHA Penning traps, was recently published³. Patch potentials are surface potentials on the interior walls of Penning trap electrodes. Such potentials, whose origin is not completely understood, build up over time on the cryogenic electrodes and have deleterious effects on antihydrogen production and trapping. The results in this article have important operational consequences for both ALPHA-2 and ALPHA-g.

The 2023 Run

The ALPHA collaboration operates two, distinct machines for production, trapping, and investigation of antihydrogen. The ALPHA-2 apparatus is mainly used for spectroscopic studies, and the ALPHA-g machine is a dedicated gravity experiment (see Fig. 1). For the 2023 experimental run, we operated only the ALPHA-2 experiment – the ALPHA-g machine was disassembled for upgrades. In particular, the ALPHA-g external solenoid was modified. The cryocoolers for this superconducting, 1 T magnet were replaced by new, higher capacity units. During the 2022 run, it was necessary to warm up and re-cool this solenoid occasionally, resulting in many days of lost beamtime. The intervention to modify the magnet was done at CERN by the manufacturer (Bilfinger). In early tests, the problem appears to be resolved, and ALPHA-g is being re-assembled at this time. This major intervention required removal of ALPHA-g from the beamline, followed by removal of the cryostat and both detectors from the solenoid. The commissioning and data-taking with ALPHA-g had been the priority for the collaboration in 2021 and 2022, although we did exercise ALPHA-2 at times to ensure its functionality.

We thus worked with only ALPHA-2 during the 2023 beamtime. This year was arguably the most productive in ALPHA history for spectroscopic measurements of antihydrogen and other achievements. We briefly describe below seven different physics results for which publications are currently in preparation.

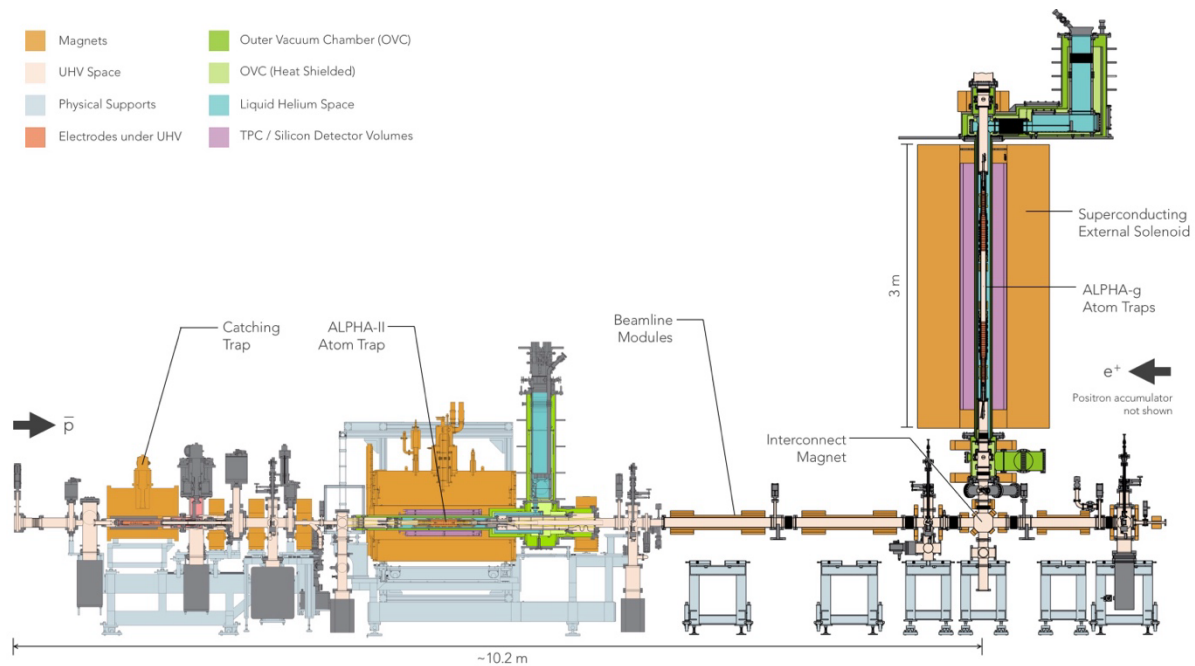


Figure 1. Schematic diagram of the ALPHA experimental zone, showing the ALPHA-2 and ALPHA-g devices. The positron accumulator is not illustrated; it is situated to the right, off of the diagram.

I. Accumulation of 10^4 hbars using laser-cooled Be ions

The purpose of this endeavour was to use trapped, laser-cooled Be ions to sympathetically cool the positrons to be used in antihydrogen production. During the past 13 years of antihydrogen trapping in ALPHA, we have observed that the positron plasma temperature as a very important factor for the production and trapping of antihydrogen. Roughly speaking, the antiprotons are believed to equilibrate rapidly in the positron plasma, setting the energy scale for the produced antihydrogen atoms. As the neutral trap has a depth of only 0.5 K; only a fraction of the atoms produced in our typical positron plasmas at 20 K can be trapped.

Several years ago, the collaboration, under the leadership of N. Madsen, undertook a program to try to obtain colder positrons by employing a mixed plasma of Be ions and positrons. The original idea⁴ is from the Bollinger group at NIST. The Be ion, chosen for its low mass, can be laser cooled using commercial lasers. The positrons are then sympathetically cooled due to the Coulomb interactions with cold Be ions. The details of this procedure are beyond the scope of this report. The team succeeded in 2023 in fully implementing this scheme in the antihydrogen production and accumulation sequence. The key result is shown in Figure 2. ‘Stacking’ refers to the process of repeatedly mixing new plasmas of antiprotons and positrons in the neutral trap to accumulate atoms of antihydrogen for some time period. We currently perform about 15 mixing cycles per hour. Figure 2 shows the evolution from the typical situation with no-Be (red points and curve) to the current state-of-the-art with Be (black triangles and curve). ‘Pass cuts’ refers to silicon vertex detector (SVD) events that meet the online criteria for antihydrogen annihilations. The accumulation rate has risen dramatically, and we have been able to have more than 10,000 atoms trapped at once. The best observed, short-term rate was for a 20-stack sequence with an average of 73 passed cuts per stack. This new technique was used for most of the results to be described below. It represents a complete paradigm shift for our physics program.

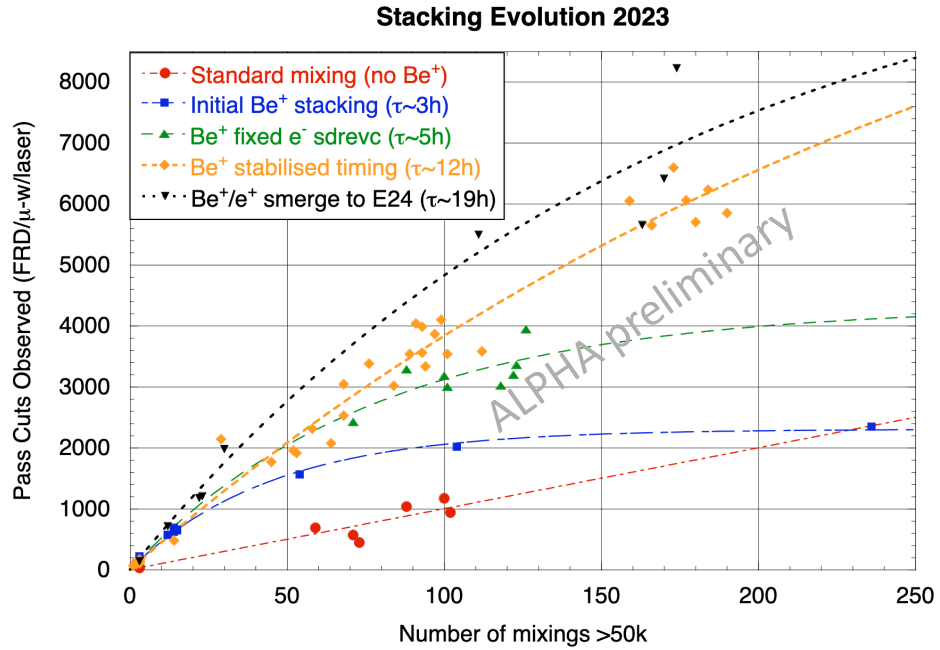


Figure 2. Stacking evolution during 2023. See the text for details. The number of pass cuts represent all antihydrogen annihilations detected during the experimental manipulations after stacking, and is corrected for annihilations on the background gas.

II. Progress on laser cooling of antihydrogen

The collaboration demonstrated laser cooling of trapped antihydrogen in a 2021 publication⁵. This was a proof of principle result demonstrating three-dimensional laser cooling with a pulsed, 121 nm, Lyman-alpha laser. In 2023 we dedicated some beamtime to more in-depth studies of the efficacy of laser cooling in ALPHA-2. Figure 3a illustrates the relevant transitions in antihydrogen. The cooling laser transition is illustrated with blue or red detuned arrows. The transition shown in black can be used to probe the resulting velocity distribution. Exciting this transition can lead to relaxation to an untrapped state, and the resulting annihilation can be detected. The lineshape of the measured 1S-2P line obtained by scanning the laser frequency holds longitudinal velocity information through Doppler broadening. By measuring the time-of-flight (TOF) between the laser pulse and the annihilation on the wall, we can also extract transverse velocity distributions. These techniques are described in detail in the original article⁵.

Figure 3b is an example of the types of measurements that were made in 2023. These curves show the time evolution of the probed linewidth during the cooling process. Note that the horizontal scale represents more than four hours. The cooling laser has a fixed detuning for the duration, but the process is stopped periodically to probe the lineshape. The probing obviously results in the loss of some of the trapped sample, so the work with Be-aided stacking described above was essential for these measurements. The curves taken in Figure 3b were typically measure after an overnight accumulation of antihydrogen, resulting in several thousand atoms in the initial population.

Figure 4 shows the time-of-flight data for a subset of the cooling runs. Note that colder atoms come out later, so the signature of cooling is that the distribution evolves to the right of these graphs.

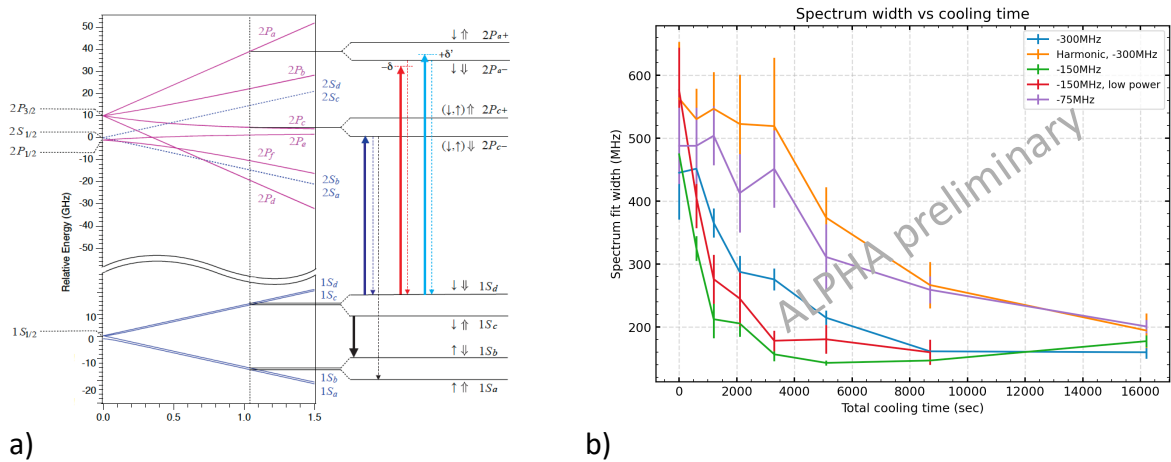


Figure 3. a) The relevant level diagram for laser cooling and probing. b) Measured 1S-2P linewidth versus cooling time for various conditions (laser detuning, power, trap potential shape).

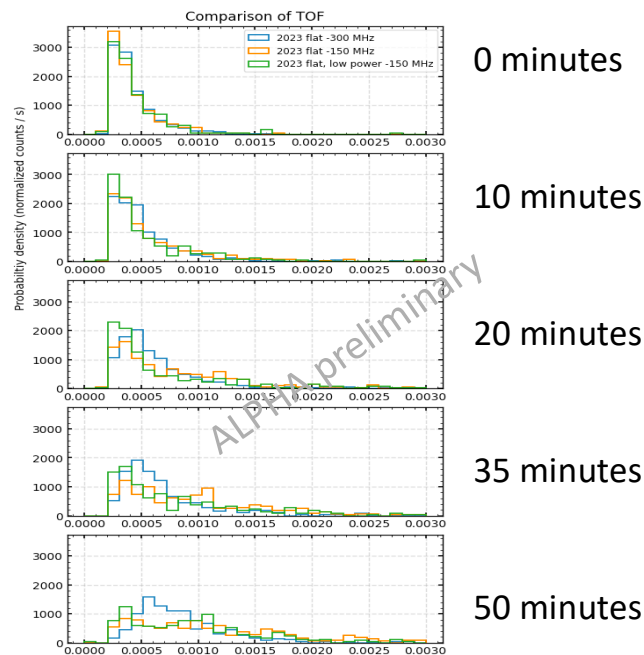


Figure 4. Time evolution of the TOF distributions during laser cooling, for various conditions. See text for details.

Finally, Figure 5 illustrates the reproducibility of the cooling process over a few runs with 300 MHz detuning. Also shown are one run with 200 MHz detuning, and a typical distribution with no cooling. The black curve is the result of a simulation that results in a mean transverse energy equivalent to 15mK in temperature units. These results are preliminary, but we have various indications that we can regularly achieve a sample of thousands of antihydrogen atoms that are laser cooled to a mean energy of 15 mK in the transverse and longitudinal degrees of freedom.

Before proceeding to the next topic, it is worth considering the operational implications of the above two sections. On a given day at the end of the 2023 run, we could

routinely begin a new stack of antihydrogen atoms, at say, 22:00, then accumulate 150-200 cycles overnight – leading to roughly 6000 detectable atoms (Figure 2). This sample would then be laser cooled for several hours, and then used for a measurement program during the afternoon. For example, a complete measurement of a 1S-2S line would take a few hours. Then the whole process would be repeated, with perhaps a completely different physics goal for the next day. Such performance was almost unimaginable when the first anti-atoms were trapped in ALPHA in 2010. Then the average was roughly one trapped atom per 8 attempts.

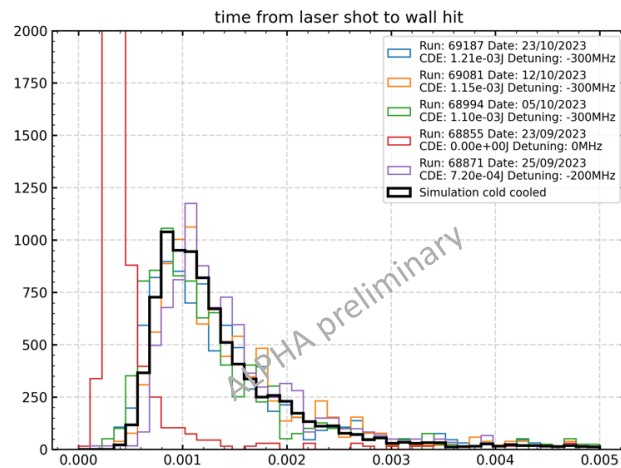
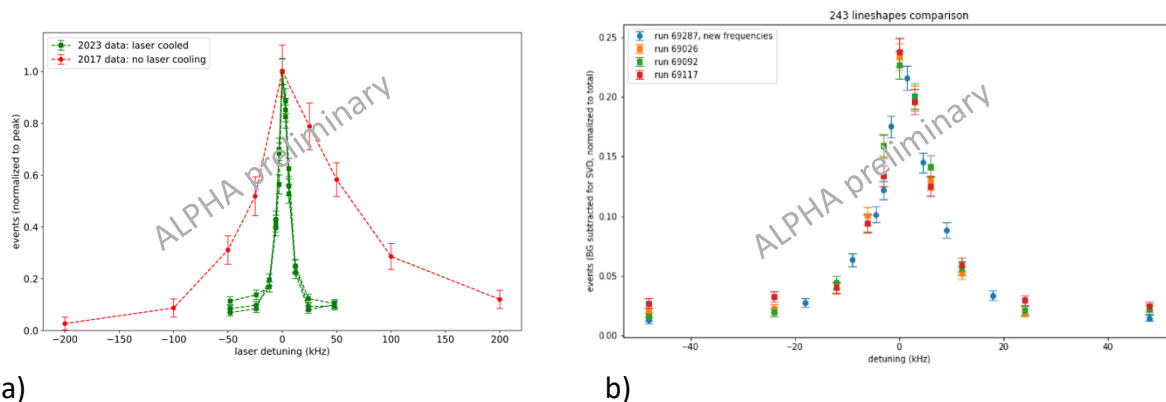


Figure 5. Various TOF distributions; see text for details.

III. the 1S-2S transition with laser cooling

A key goal of ALPHA has always been precision study of the 1S-2S transition in antihydrogen. We have previously made a frequency measurement that is consistent with expectations for hydrogen with a precision of a few parts per trillion⁶. We have continued to study this transition in 2023, profiting from the large sample sizes and cold temperatures described above. The analysis of the data for 2023 is in the very early stages, but we present some essentially raw data in Figure 6. Figure 6a) shows the 2023 raw data plotted along with an earlier result – without laser cooling - from 2017. Figure 6b) shows several spectra taken in 2023 to illustrate the measured lineshape and linewidth, as well as the repeatability of the measurements. The frequency scale is relative; an absolute determination has not yet been performed.



a) b) **Figure 6.** Measured spectra of the 1S-2S transition in antihydrogen. See text for details. Note the different normalization for the two graphs.

Pending the detailed analysis, we are optimistic that the new data represent an important step forward for this measurement. We also note that the ALPHA Metrology Laboratory, featuring the hydrogen maser and the cesium fountain clock, was commissioned and operational for the 2023 measurements. See the slides for some technical details on the performance of this system.

IV. Excited state spectroscopy: the 2S-2P transition

As it is now routine to excite the 1S-2S transition in antihydrogen in ALPHA, it is natural to consider further excitation from the metastable 2S state. In 2023 we took the first step in this direction, by performing double resonant excitation: first from the 1S to the 2S state using two photons from the 243 nm laser, and then to a 2P state using microwaves. The relevant level diagram appears in Figure 7a. We utilize the transition $1S_d$ to $2S_d$, and park the laser near the resonant maximum. Microwaves can then excite the levels $2P_f$ or $2P_a$, depending on the frequency chosen. The subsequent fate of the excited atoms is quite different: the $2P_f$ state relaxes to the untrapped $1S_b$ state, whereas the $2P_a$ state decays to the trapped $1S_d$ state. Thus, in the current conditions in ALPHA, compared to the situation without microwaves, the $2P_f$ path enhances the loss of antihydrogen from the trap, while the $2P_a$ branch suppresses loss. An example of this behaviour is shown in Figure 7b, with the two levels indicated. Again, the data analysis is in the very early stage, but this curve represents the first excited state spectroscopy of an anti-atom. We have repeated this measurement for various microwave powers and magnetic fields.

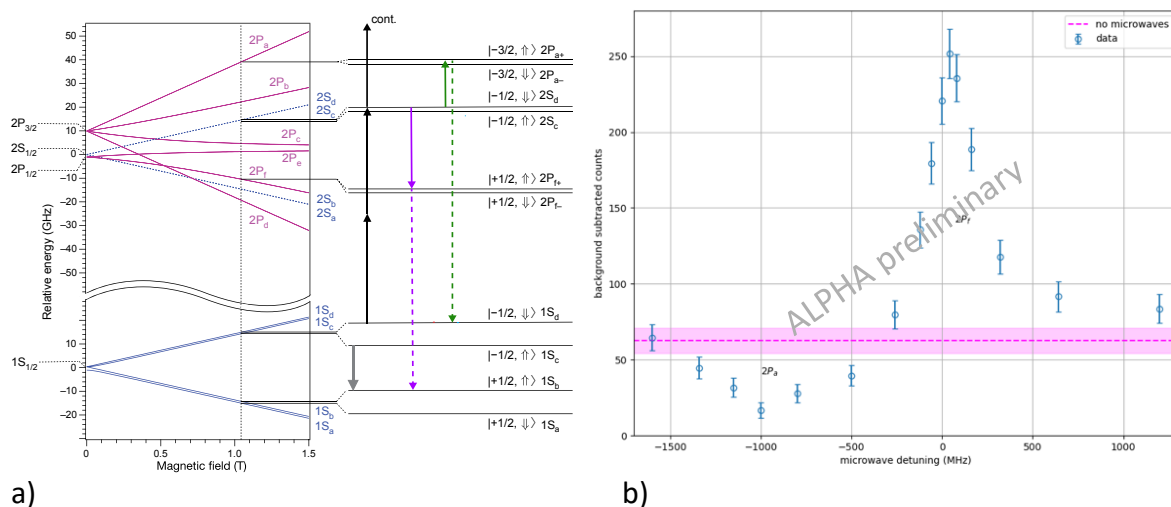


Figure 7. a) Relevant levels for double resonant spectroscopy in antihydrogen. b) A sample spectrum taken by scanning the microwave frequency at fixed 243 laser frequency.

V. Positron spin resonance: ground state hyperfine splitting (GSHFS)

We have previously studied the ground state hyperfine structure in antihydrogen using microwave-induced spin flips and annihilation detection^{7,8}. The Breit-Rabi diagram is shown in Figure 8a. Microwaves can resonantly drive the transitions $1S_d$ to $1S_a$, or $1S_c$ to $1S_b$. The difference between these two frequencies gives the ground state hyperfine splitting. Figure 8b shows an example spectrum of atoms ejected due to this resonance. The microwave frequency is scanned from low to high, first ejecting the C-state atoms and then the D-state

ones. Note there is a frequency jump between the two peaks – the scan is linear in time for each peak.

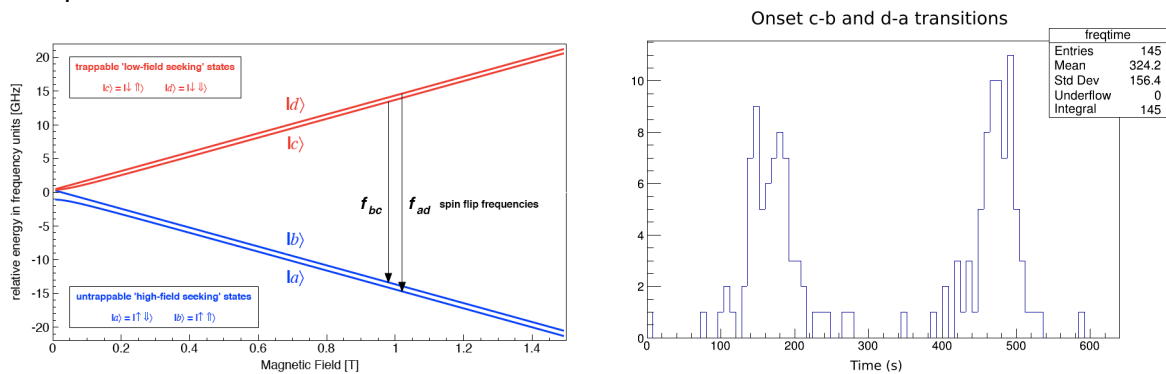


Figure 8. a) The Breit-Rabi diagram showing the transitions from trapped (red) to untrapped (blue) levels. b) A microwave frequency scan across the two transitions. Note that the abscissa is time and there is a frequency jump between the two distributions.

Our earlier measurement resulted⁸ in an uncertainty in the GSHFS of a few parts in 10^4 . Some of the data collected in 2023 are shown in Figure 9. Here, the onset frequency (corresponding to the magnetic minimum in the trap) determined for each transition is plotted as a function of time as the persistent field in the ALPHA-2 solenoid slowly decays. Note that this experiment was mostly done early in the run, before the implementation of the Be stacking. Each pair of points represents 10 stacks and ~ 150 atoms. The 2023 data are currently being analyzed. It is not unreasonable to expect a GSHFS frequency precision of a few ppm from these data. Note in passing that the microwave interaction allows us to eject one or other of the trapped states. We have utilized this state selection in many other experiments, as described above.

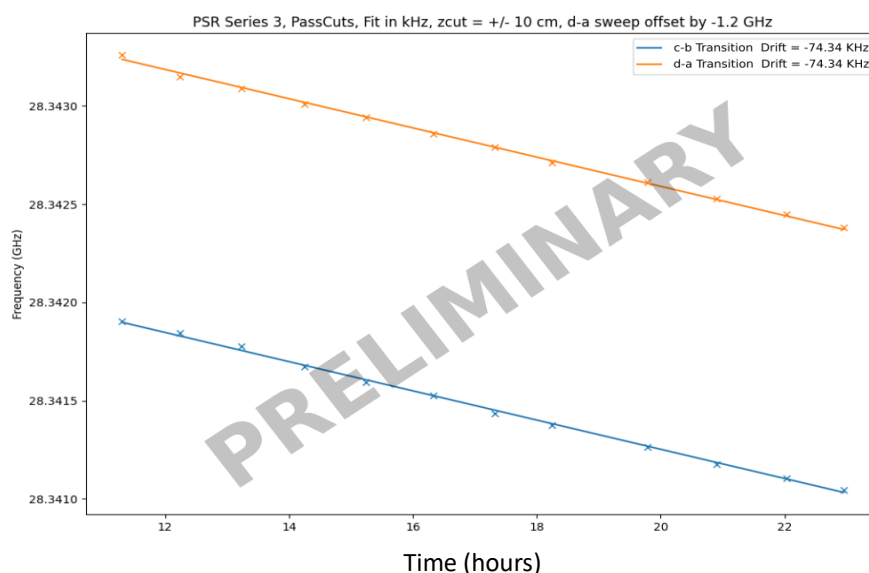


Figure 9. Evolution of the onset frequencies for the two hyperfine transitions due to the slow change of the persistent field.

VI. MCP detection for spectroscopy experiments

All of our spectroscopic measurements are based on resonant loss of antihydrogen and detection of its annihilation. The detection is by the ALPHA-2 silicon vertex detector. In 2023, we investigated an alternative to this detection method. The new method, suggested by S. Jones, involves a multichannel plate (MCP) detector and is relevant when the resonant loss is due to antihydrogen annihilation. Figure 10a illustrates the Penning trap and magnetic trap structures in ALPHA-2, as well as the SVD. Normally during spectroscopy measurements, the Penning trap electrodes are de-energised to avoid unwanted electric fields. However, it is possible to configure an axial potential well such that antiprotons from antihydrogen ionization would be captured (the axial magnetic field from the solenoid is always present). These antiprotons can then be accelerated and extracted along the axis to be detected by an MCP (not pictured in Fig. 10). A typical measurement would then involve exposing a trapped antihydrogen sample to a particular radiation frequency for some time while collecting the ionized antiprotons, and then extracting the antiprotons to the MCP before incrementing the frequency and repeating the process.

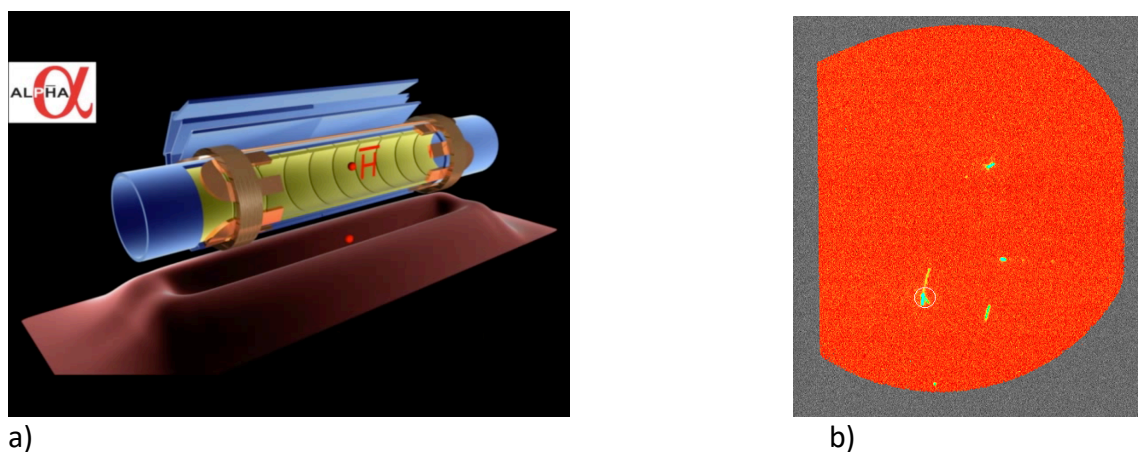


Figure 10. a) Cutaway schematic of the ALPHA-2 Penning and atom traps, illustrating the magnetic potential well that traps antihydrogen. The SVD layers are also shown. The MCP is not pictured. b) camera image of the MCP's phosphor screen illustrating the signal from a few extracted antiprotons. In practice, a silicon photomultiplier is used to count the antiprotons.

Figure 11 shows a 1S-2S spectrum obtained using this technique, in comparison with the usual method using the SVD. We have very limited experience with this technique so far, but the early results are very promising. Significantly, this technique would also be applicable to *hydrogen* atoms trapped in ALPHA. It has long been a goal of the collaboration to trap hydrogen atoms in the same volume and to study their spectrum under ALPHA conditions. The obvious advantage to understanding systematic effects can not be overestimated.

VII. Energy diagnostics using octupole ramp-down

Finally, we consider a new technique to study the kinetic energy distribution of trapped antihydrogen atoms in various scenarios. Referring to Figure 11a, this technique, implemented and studied by D. Hodgkinson, involves ramping down the current in the octupole magnet to release the trapped antihydrogen atoms transversely. Both the time and position distributions of the resulting annihilation events carry information about the energy distribution of the trapped sample. In practice, the data from such experiments can be

compared to simulations and to, for example, the Lyman-alpha velocity measurements described above

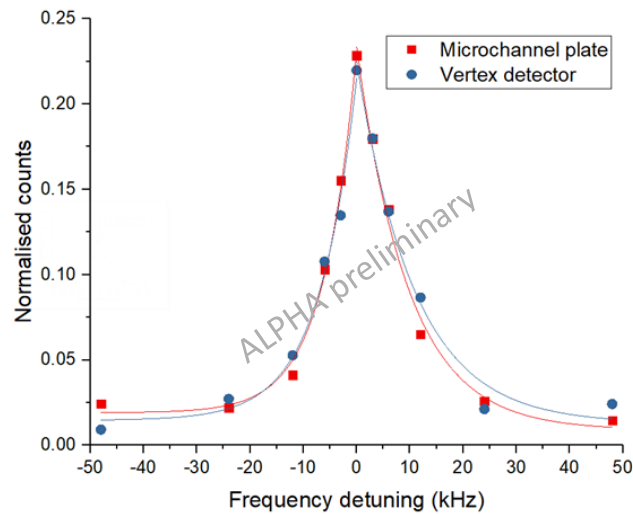


Figure 11. The lineshape of a 1S-2S transition measured with the new MCP technique (red) and with the traditional SVD (blue).

Figure 12 shows some distributions extracted using this technique, which internally goes by the name of “Fast Ramp Down” or FRD. In practice, “fast” is 15 seconds or more. We typically use temperature units to quantify the energetics in the 500 mK deep confinement well. For precision spectroscopy and for gravitational studies, it is obviously of utmost importance to understand as much as possible about the energy distribution of the trapped anti-atoms. We are confident that the FRD method holds a lot of promise both in analyzing such results and in benchmarking and informing our detailed computer simulations of antihydrogen dynamics in the trap. Early results show a good agreement between the FRD and TOF methods (Fig.12).

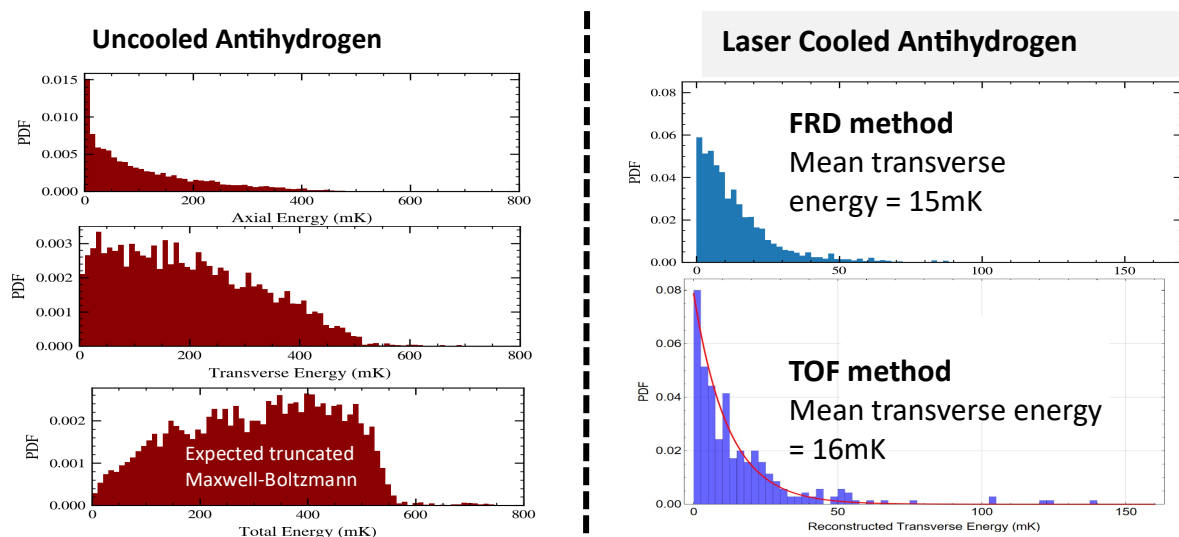


Figure 12. Energy distributions for uncooled antihydrogen obtained by FRD (left, top and middle). The bottom panel represents the expected energy distribution if the atoms are

selected from an MB distribution truncated at the trap depth. (right) The transverse energy distribution of laser cooled antihydrogen as determined by FRD and the TOF methods.

Summary and outlook

The 2023 run was extremely productive for the collaboration, due in no small part to the reliability of the AD/ELENA complex. The ALPHA-2 activities continued 24/7 for the entire run, as is the tradition in ALPHA. For 2024 we expect to alternate between ALPHA-2 and ALPHA-g operations, although the distribution of time has yet to be decided. For ALPHA-2, we will improve the above measurements and techniques as dictated by the ongoing analysis, and perhaps begin to investigate other transitions, such as the 2S-3S or the 2S-4P. For ALPHA-g, the tasks on the horizon include implementing laser cooling and Be-stacking as demonstrated in ALPHA-2. We will also begin to commission the other two antihydrogen traps that are part of ALPHA-g. A new fixed helium transfer line recently installed in ALPHA-g will hopefully decrease the liquid helium consumption to more manageable levels, but this line has yet to be tested.

We thank the AD/ELENA team for a very productive year.

¹Anderson, E. *et al.* Observation of the effect of gravity on the motion of antimatter, *Nature* **621** (2023).

² Baker, C., *et al.* Precision spectroscopy of the hyperfine components of the 1S-2S transition in antihydrogen, red to be published in *Nature Physics* (2024).

³ Baker, C.J., *et al.* The effects of patch potentials in Penning-Malmberg Traps, *Phys. Rev. Research* **6**, L012008 (2024).

⁴ Jelenkovic, B. M. *et al.* Sympathetically cooled and compressed positron plasma. *Phys. Rev. A* **67**, 063406 (2003).

⁵ Baker, C.J., *et al.* Laser cooling of antihydrogen atoms. *Nature* **592**, 35–42 (2021).

⁶ Ahmadi, M. *et al.* Characterization of the 1S–2S transition in antihydrogen. *Nature* **557**, 71–75 (2018).

⁷ Amole, C. *et al.* Resonant quantum transitions in trapped antihydrogen atoms. *Nature* **483**, 439–443 (2012).

⁸ Ahmadi, M. *et al.* Observation of the hyperfine spectrum of antihydrogen. *Nature* **548**, 66–69, (2017).